AJNR

Quantitative Susceptibility Mapping of Time-Dependent Susceptibility Changes in Multiple Sclerosis Lesions

S. Zhang, T.D. Nguyen, S.M. Hurtado Rúa, U.W. Kaunzner, S. Pandya, I. Kovanlikaya, P. Spincemaille, Y. Wang and S.A. Gauthier

AJNR Am J Neuroradiol 2019, 40 (6) 987-993
doi: https://doi.org/10.3174/ajnr.A6071
http://www.ajnr.org/content/40/6/987

Quantitative Susceptibility Mapping of Time-Dependent Susceptibility Changes in Multiple Sclerosis Lesions

S. Zhang, T.D. Nguyen, S.M. Hurtado Rúa, U.W. Kaunzner, S. Pandya, I. Kovanlikaya, P. Spincemaille, Y. Wang, and S.A. Gauthier

ABSTRACT

BACKGROUND AND PURPOSE: MR imaging studies have demonstrated that magnetic susceptibility in multiple sclerosis lesions is dependent on lesion age. The objective of this study was to use quantitative susceptibility mapping to determine whether lesions with a hyperintense rim, indicative of iron-laden inflammatory cells (rim+), follow a unique time-dependent trajectory of susceptibility change compared with those without (rim−).

MATERIALS AND METHODS: We studied patients with MS with at least 1 new gadolinium-enhancing lesion and at least 3 longitudinal quantitative susceptibility mapping scans obtained between 1.1 and 6.1 years. Lesions were classified as rim+ if a hyperintense rim appeared on quantitative susceptibility mapping at any time. A multilevel growth curve model compared longitudinal susceptibility among rim+ and rim− lesions.

RESULTS: Thirty-two new gadolinium-enhancing lesions from 19 patients with MS were included, and 16 lesions (50%) were identified as rim+. Quantitative susceptibility mapping rim+ lesions were larger than rim− lesions with gadolinium enhancement ($P < .001$). Among all lesions, susceptibility increased sharply after enhancement to a peak between 1 and 2 years followed by a decrease. The overall susceptibility curve height for rim− lesions was 4.27 parts per billion lower than that for rim+ lesions ($P = .01$). Rim− lesions demonstrated a higher linear slope relative to rim+ lesions ($P = .023$) but faster cubic decay relative to rim+ lesions ($P = .005$). Rim− lesions started decaying approximately 2 years earlier compared with rim+ lesions.

CONCLUSIONS: There was a marked difference in the susceptibility temporal trajectory between rim+ and rim− lesions during the first 6 years of lesion formation. Most rim+ lesions retain iron for years after the initial lesion appearance.

ABBREVIATIONS: Gd = gadolinium; Gd+ = Gd-enhancing; GRE = gradient recalled-echo; QSM = quantitative susceptibility mapping; ppb = parts per billion; rim+ = rim positive; rim− = rim negative

Quantitative susceptibility mapping (QSM)[1] provides efficient in vivo quantification of susceptibility changes related to iron deposition and helps identify lesions with iron-laden inflammatory cells.[2] It has been widely used in studying multiple sclerosis and can demonstrate the retention of iron among a subset of chronic lesions.[3-5] Enhancing MS lesions identified on post-gadolinium (Gd) T1WI in the routine MR imaging surveillance are representative of the breakdown of the blood-brain barrier and acute disease activity.[6] As the BBB closes, lesions transition to the chronic stage. However, a subset of lesions may retain a rim of iron-enriched inflammatory cells with ongoing damage. Chronic active MS lesions, characterized by a hyperintense rim on QSM, have been shown to contain iron-enriched, activated microglia and macrophages on histopathology[5] and have been linked to greater tissue damage on in vivo MR imaging.[7,8] Identifying lesions likely to retain chronic inflammation would be useful for potential therapeutic targeting. Accordingly, it would be valuable to study MS lesion-evolution trajectories from the time of enhancement to the chronic lesion stage.

QSM is a phase-based magnetic field deconvolution technique that overcomes blooming artifacts and provides accurate quanti-

Received January 29, 2019; accepted after revision April 17.

From the Departments of Radiology (S.Z., T.D.N., S.P., I.K., P.S., Y.W., S.A.G.) and Neurology (U.W.K., S.A.G.) and Feil Family Brain and Mind Research Institute (S.A.G.), Weill Cornell Medicine, New York, New York; Department of Radiology (S.Z.), Tongji Hospital, Tongji Medical College, Huazhong University of Science and Technology, Wuhan, China; Department of Mathematics and Statistics (S.M.H.R.), College of Science and Health Professions, Cleveland State University, Cleveland, Ohio; and Department of Biomedical Engineering (Y.W.), Cornell University, Ithaca, New York.

This work was supported, in part, by grants from the National Institutes of Health (R01NS090464, R01NS104283, R01NS105144, S10 OD021782), the National Multiple Sclerosis Society (RG-1602-07671), and grant UL1 TR000456-06 from the Weill Cornell Clinical and Translational Science Center.

Please address correspondence to Susan A. Gauthier, DO, MPH, Department of Neurology, Weill Cornell Medical College, 1305 York Ave, Suite Y217, NY, NY 10021; e-mail: sag2015@med.cornell.edu

http://dx.doi.org/10.3174/ajnr.A6071

fication and localization of the magnetic sources.[1,9,10] Previous QSM studies demonstrated that MS lesion susceptibility increases as the acute, enhancing MS lesion transitions to the nonenhancing stage, reaches a peak in the chronic active stage, and eventually decays away in the final stage of a glia scar.[11-14] Although these studies identified a unique time-dependent trajectory in susceptibility on QSM, they are limited given the cross-sectional design or short longitudinal follow-up. In addition, a number of recent gradient recalled-echo (GRE) imaging studies have identified a unique subpopulation of chronic MS lesions with a hypointense rim on the phase image or a hyperintense rim on QSM. These studies have used histopathologic validation[7,15-17] and, more recently, PET imaging[18] to validate that these lesions have persistent inflammation represented by iron-laden microglia and macrophages. Initial detection and the expected life span of lesions with a hyperintense rim appearance on QSM (rim+) as well as the time-dependent susceptibility changes among these lesions compared with those without a rim (rim−) have yet to be explored, to our knowledge.

The aim of this study was to assess longitudinal tissue-susceptibility changes in new Gd-enhancing lesions for up to 6 years after the first identification and to determine whether lesion trajectories depend on the development of a hyperintense rim on QSM.

MATERIALS AND METHODS

Patient Selection

This was a retrospective study of a cohort of 19 patients with relapsing-remitting MS selected from an ongoing, prospective MS MR imaging and clinical data base for which annual MR imaging scans (including QSM) were collected during 6 years. Patients were selected for this study if they met the following inclusion criteria: 1) They had at least 1 new Gd-enhancing (Gd+) MS lesion on routine annual MR imaging, 2) had at least 3 longitudinal QSM scans (including at the time of Gd+ lesion detection), 3) had at least 1 MR imaging performed >1 year after Gd+ lesion detection, and 4) had prior MR imaging to ensure that Gd+ lesions were newly formed lesions and not re-enhancement of older lesions. MR images were acquired on 2 different imaging platforms during the 6 years (GE Healthcare and Siemens, details below). Clinical data collected for patients included the following: age, sex, Expanded Disability Status Scale scores, disease duration, and treatment duration. This study was approved by Weill Cornell Medicine institutional review board, and written informed consent was obtained from each subject.

MR Imaging Protocol and Image Processing

Brain MRIs (from 2011 to 2018) were performed on 3T MR imaging scanners (Signa HDxt, GE Healthcare, Milwaukee, Wisconsin, with a product 8-channel head coil; Magnetom Skyra, Siemens, Erlangen, Germany with a product 20-channel head/neck coil). The scanning protocol consisted of standard 3D-T1WI, 2D-T2WI, and 3D-T2-weighted FLAIR sequences for anatomic structure, multiecho 3D-GRE imaging for QSM, and gadolinium-enhanced 3D-T1WI to detect blood-brain barrier disruption. The acquisition parameters for multiecho GRE were the following: FOV = 24 cm, TR = 49–58 ms, TE1/ΔTE = 4.5–6.7/4.1–4.8 ms, last TE = 47.7 ms, acquisition matrix = 320–416 × 205–320, readout bandwidth = 244–260 Hz/pixel, axial slice thickness = 3 mm, flip angle = 15°–20°, acceleration factor = 2, number of averages = 1. The scan time was around 4 minutes and 30 seconds (48 slices), varying slightly with brain superior-inferior dimensions.

This QSM imaging protocol was harmonized for both scanner manufacturers and was demonstrated to be reproducible across manufacturers.[19,20] QSM was reconstructed from complex GRE images using a fully automated morphology-enabled dipole inversion (MEDI+0) method zero-referenced to the ventricular CSF.[21] All the conventional images (T1WI, T1WI+Gd, T2WI, T2-weighted FLAIR) and the follow-up QSM images were coregistered to the baseline GRE magnitude images using the FMRIB Linear Image Registration Tool (FLIRT; http://www.fmrib.ox.ac.uk/fsl/fslwiki/FLIRT).[22]

Lesion Susceptibility and Volume Measurements

New Gd+ MS lesions were identified on T1WI+Gd images and visually classified on QSM as rim+ or rim−[8] by 2 independent reviewers (S.Z., a neuroradiologist with 7 years of experience; S.A.G., an MS neurologist with 16 years of experience).[8] A lesion was designated as rim+ if QSM was hyperintense at the edge of the lesion at any of the longitudinal time points. In addition, at each time point, newly identified Gd+ lesions were dated as zero years. Lesions were also classified as either "nodular" or "shell" enhancing to estimate the stage of lesion enhancement (ie, early or late stage, respectively).[12,23] In case of a rare (4 lesions) disagreement, a third neuroradiologist (I.K., with 22 years of experience) determined the lesion type. ROI analysis was performed using ITK-SNAP software (Version 3.6.0; http://www.itksnap.org/) to obtain regional volume and QSM measurements within the identified lesions. To assess a change in lesion volume, we drew lesion ROIs on raw T2-weighted FLAIR images, which had isotropic 1-mm high-resolution images, at all time points. To assess longitudinal susceptibility change, we first created ROIs on coregistered T2-weighted FLAIR images and then overlaid them on the QSM images at initial lesion detection. When necessary, these ROIs were manually edited to better match lesion geometry on QSM and removal of the central veins (vessel-like structures with hyperintense QSM appearance). The edited ROIs were overlaid onto QSM images from all other subsequent time points. The susceptibility value of the adjacent normal-appearing white matter was subtracted from the lesion susceptibility to offset the influence of local fiber orientation.

Statistical Analysis

A regression model with orthogonal time polynomials was used to analyze the longitudinal evolution of lesion volumes for rim+ and rim− lesions at the lesion level while adjusting for multiple lesions per patient. The final model included a third-order orthogonal polynomial, the fixed conditional effect was lesion group, and patient was the random effect.

A multilevel growth curve model with orthogonal time polynomials was used to analyze the longitudinal evolution of QSM values for rim+ and rim− lesions while adjusting for patient-level covariates (fixed effects: individual lesion volume, patient age, Expanded Disability Status Scale score, disease duration, and

treatment duration) and multiple lesions per patient (random effects). An eighth-order orthogonal polynomial model was necessary to capture the upward and downward evolution of QSM values within lesion groups. Orthogonal polynomials are transformations that make the original time terms independent. They allow a precise and robust evaluation of QSM longitudinal differences. Our orthogonal polynomial was defined on the basis of the lesion-age octiles (8 quantiles). This approach accounts for the sample lesion age distribution. The statistical analysis was performed using R statistical and computing software (2017; http://www.r-project.org/).

RESULTS

Patient and Lesion Characteristics

Nineteen patients with relapsing-remitting MS (15 women and 4 men, 36.3 ± 6.4 years of age) met the inclusion criteria with a total of 32 new T1WI+Gd lesions: 9 nodular-enhancing (28%, susceptibility, 6.87 ± 5.80 parts per billion [ppb]) and 23 shell-enhancing (72%, 12.10 ± 8.95 ppb) lesions. Central veins were found in 10 (31%) lesions. Patients had a mean disease duration of 4.8 ± 3.2 years and an Expanded Disability Status Scale score of 1.4 ± 1.7. The average time from initial MR imaging to the last MR imaging was 3.6 ± 1.4 years (range, 1.1–6.1 years). Patients were treated with various disease-modifying therapies, and at the time of lesion identification, the cohort was on therapy for a mean duration of 3.5 ± 3.0 years.

Lesions with a Hyperintense Rim on QSM

Among the 32 new Gd+ lesions, 16 lesions (50%) were identified as QSM rim+, and evidence of the rim was seen at the time of enhancement for most (81%) of these lesions. Qualitatively, rim+ lesions were visualized on QSM scans longer than rim− lesions (Figs 1–3), and once identified, the hyperintense rim was consistently found on all subsequent scans in 14 (88%) of the rim+ lesions (Figs 2 and 3). Although susceptibility values were lowest at the time of Gd-enhancement, subtle evidence of a rim could be seen in 13 (81%) lesions at that time. The longitudinal evolution of lesion volume, adjusting for multiple lesions per patient and conditioning on lesion group, is presented in Fig 4. Fitted volumes derived from the regression model demonstrated that rim+ lesions (1042.45 mm^3) were significantly larger than rim− lesions (322.34 mm^3) at the time of Gd-enhancement ($P < .001$). Following the start of a decline in volume after Gd-enhancement, rim+ lesions remained larger than rim− lesions and maintained a significant difference at lesion ages 0.5, 2, and 4 years (all $P < .001$) (Fig 4).

Time-Dependent Susceptibility Change in QSM Rim+ and Rim− Lesions

The final model for the longitudinal lesion evolution of QSM values included T2-weighted FLAIR lesion volume and Expanded Disability Status Scale scores at baseline as patient-level fixed effects (all P values $< .05$). All lesions demonstrated a continued increase in susceptibility until a peak between 1 and 2 years, which was followed by a reduction during the subsequent years. There was a significant effect of lesion group (rim+ versus rim−) on the intercept term, indicating lower overall QSM values for the rim− lesions relative to the rim+ (estimate = −4.27, SE = 1.62, $P = .01$) (Fig. 5). There was also a significant effect of lesion group on the slope and cubic terms, indicating a faster linear growth rate for rim− lesions relative to rim+ lesions (estimate = 8.42, SE = 3.66, $P = .023$) as well as significantly faster cubic decay for rim− lesions relative to rim+ lesions (estimate = −10.64, SE = 3.75, $P = .005$). All other effects of lesion group conditioning on time decay were not significantly different between the 2 groups. When considering lesion-volume change, as opposed to baseline lesion volume, as a covariate in the model, a significant association was found between QSM change and volume change ($P = .002$) (for every 1-mm^3 decrease in volume, there was 0.014-ppb reduction in QSM). The relationship between susceptibility and volume change was similar among rim+ and rim− lesions ($P > .27$).

The Table summarizes the model-fitted mean susceptibilities along with their 95% confidence intervals. The estimated suscep-

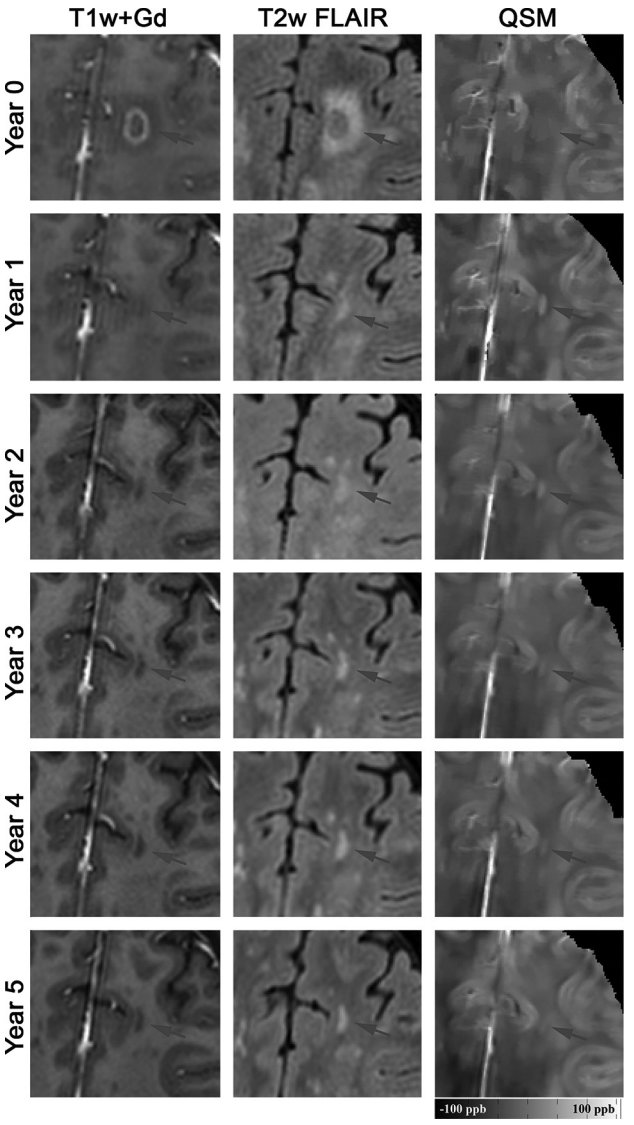

FIG 1. Longitudinal QSM and T2-weighted FLAIR images of a new Gd-enhancing MS lesion without a QSM rim appearance (rim−). At baseline, the enhancing lesion was isointense on QSM (mean lesion susceptibility = −3.31 ppb), became most hyperintense at 1 year (22.50 ppb), and gradually disappeared in subsequent years (−1.18 ppb at year 5).

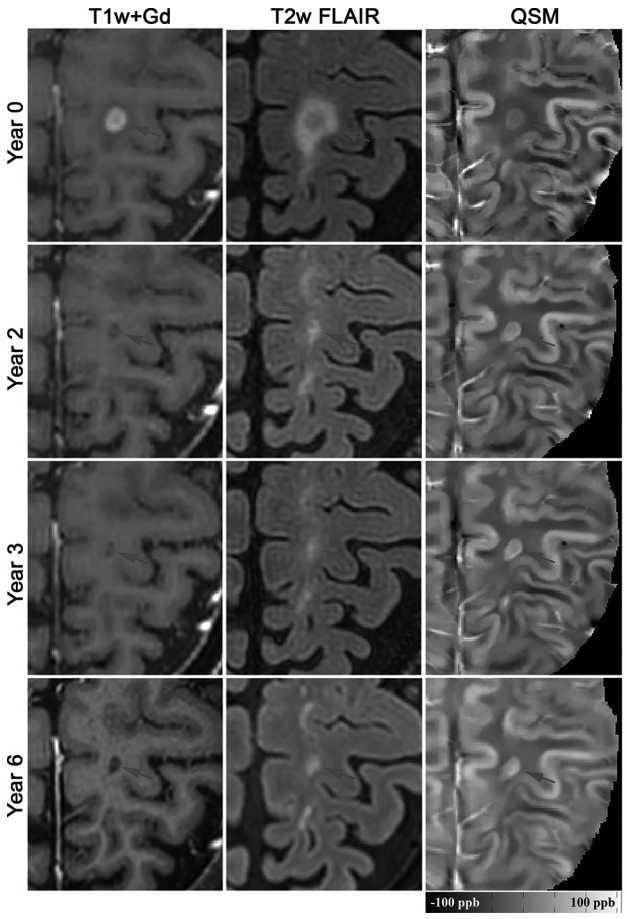

FIG 2. Longitudinal QSM and T2-weighted FLAIR images of a new Gd-enhancing MS lesion with a QSM rim appearance (rim+). This lesion was slightly hyperintense on QSM at the time of Gd-enhancement (mean lesion susceptibility = 12.74 ppb), became most hyperintense at 3 years (34.28 ppb), and remained hyperintense at 6 years (25.15 ppb).

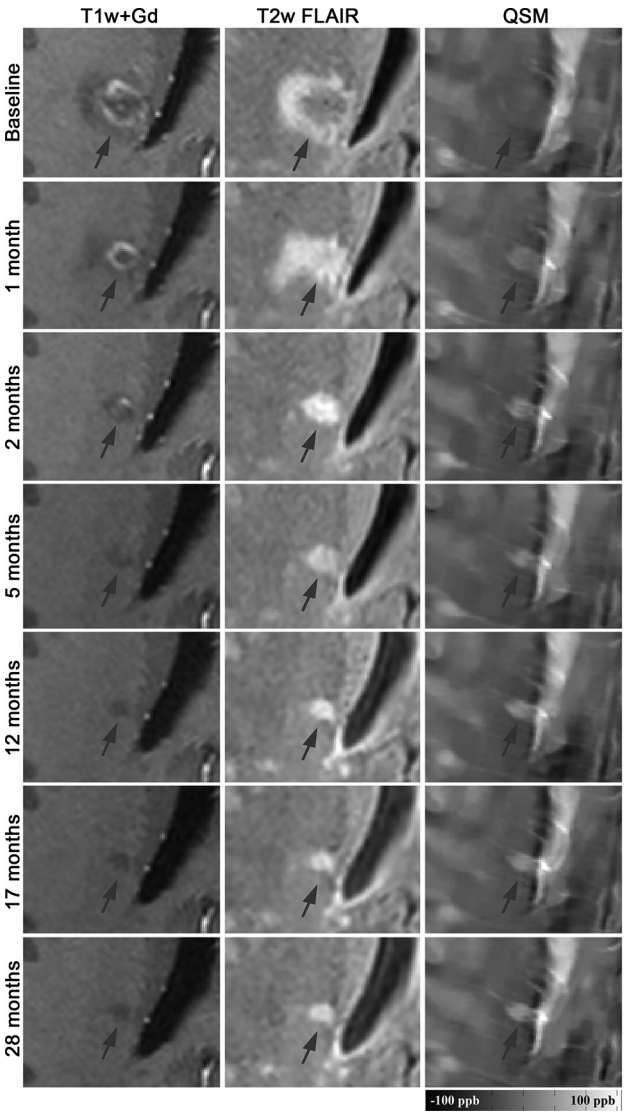

FIG 3. Longitudinal QSM and T2-weighted FLAIR images of a new Gd-enhancing MS lesion with a QSM rim appearance (rim+). This lesion was isointense on QSM at baseline and demonstrated an increase in susceptibility and rim appearance on subsequent QSM scans. The lesion susceptibility increased continually from −0.34 ppb at baseline to 26.35 ppb at 28 months. Gd-enhancement remained in this lesion until month 2.

tibility means for rim− lesions demonstrated a decay after 1.5 years with 95% confidence, while the estimated means for rim+ lesions remained persistently elevated from lesions 0.5–4 years of age. A decline in susceptibility is found in rim+ lesions only after the fourth year.

DISCUSSION

The current study is the longest longitudinal lesion-based susceptibility study examining the time-dependent susceptibility changes quantified on QSM. Our study indicates that QSM rim+ lesions have a unique time-dependent trajectory. Compared with QSM rim− lesions, rim+ lesions start with a higher susceptibility and larger volume and, most important, retain a high-susceptibility value for a number of years after initial detection. This study provides further insight into a distinct subgroup of MS lesions, those that retain a rim of iron-laden inflammatory cells and have the potential for continued tissue damage.[7,8,17]

QSM provides a noninvasive way to quantify the susceptibility change in MS lesions. The susceptibility increase observed in our study is consistent with previous studies in which a jump in lesion susceptibility occurs as an enhancing lesion evolves to the chronic, nonenhancing state.[11-14] The initial rise in susceptibility, occurring within weeks, in active lesions may be related to myelin digestion,[24] and the subsequent increase, which occurs for months, is more likely related to removal of the myelin debris within macrophages[25] and the release of iron.[12] A subset of chronic MS lesions, identified as chronic active or slowly expanding lesions, has been described as having a hypocellular lesion center and a rim of activated proinflammatory microglia and macrophages.[17,26,27] These lesions demonstrate evidence of active demyelination and axonal destruction at their rim and are thought to contribute to long-term, ongoing tissue damage in MS.[8,17,26-28] A number of studies have demonstrated that most microglia and macrophages found at the rim of chronic active MS lesions contain iron.[7,15,17,29-32] The source of the released iron is presumed to be derived from damaged myelin and dying oligodendrocytes in acute lesions[31] and functions to promote polarization of microglia and macrophage cells to a proinflammatory state.[30] Our data suggest that the development of rim+ lesions

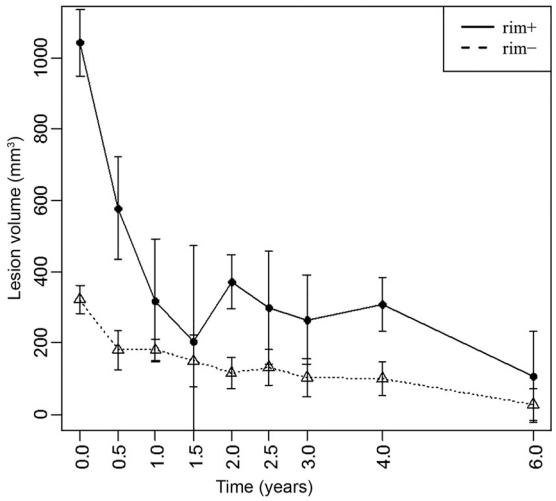

FIG 4. Longitudinal lesion-volume evolution changes among QSM rim+ and rim− lesions. Rim+ lesions were statistically larger at Gd-enhancement (time = 0), 0.5, 2, and 4 years (all $P < .0001$).

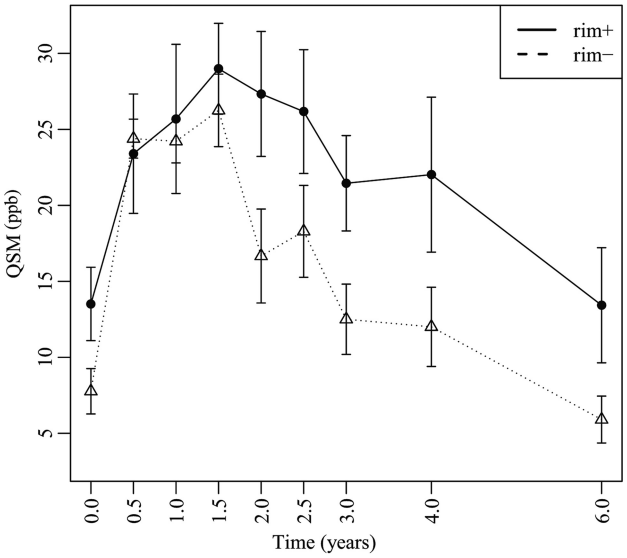

FIG 5. Longitudinal lesion age-dependent susceptibility time course of QSM rim+ and rim− MS lesions. Rim+ lesions demonstrate a higher peak QSM value and significantly slower decay rate compared with rim− (see text).

The mean susceptibility of rim+ and rim− lesions derived from the regression model

	Rim+			Rim-		
Time (yr)	No. of Lesions	Mean (ppb)	95% CI	No. of Lesions	Mean (ppb)	95% CI
0	16	13.51	11.09–15.93	16	7.77	6.27–9.26
0.5	10	23.40	19.47–27.33	9	24.39	23.11–25.67
1	7	25.69	20.78–30.60	11	24.22	22.79–25.64
1.5	5	28.99	26.00–31.98	5	26.25	23.86–28.63
2	6	27.33	23.22–31.44	7	16.66	13.57–19.76
2.5	8	26.17	22.10–30.25	10	18.29	15.27–21.31
3	7	21.45	18.31–24.59	9	12.50	10.19–14.81
4	8	22.02	16.92–27.12	10	12.00	9.40–14.61
6	5	13.42	9.64–17.21	6	5.90	4.36–7.45

may be related to a higher level of iron release, given the higher susceptibility peak among these lesions, and that the extent of iron release potentially contributes to the development of chronic inflammation. In addition, we found that rim+ lesions were much larger at the time of Gd-enhancement, a finding that supports the concept of a larger inflammatory event leading to more demyelination and iron release. Studying the physiologic mechanisms driving iron release within the acute lesion could identify therapeutic targets aimed at decreasing the occurrence of chronic active MS lesions.

The reduction of susceptibility in both rim+ and rim− lesions was related to volume loss; however, the relationship was similar and suggests that pathologic differences may explain our observed differences in the decay rate. The relatively abrupt reduction in susceptibility found among the QSM rim− lesions would be consistent with either loss of iron from the lesion or, more likely, a higher potential for remyelination among these lesions.[5] Remyelination occurring in rim− lesions would be consistent with histologic observations indicating that iron-enriched microglia and macrophages are not found at the rim of remyelinated or shadow plaques[17] and in vivo MR imaging studies demonstrating less tissue damage in lesions without a QSM rim.[7,8]

The slow decay of susceptibility in rim+ lesions and retention of the hyperintense rim suggest that these lesions retain iron for a number of years; thus, they have the potential for ongoing damage across a more extended period.[17] Although iron is retained, there is an eventual reduction in susceptibility, which suggests that most of these lesions have a life span of only a few years before iron loss and probable transition to a chronic inactive state or glia scar.[25] Histologically, chronic active lesions have been found to be associated with longer disease duration and to predominantly occur in progressive disease, in which new Gd+ lesions are infrequently found.[27] However, given the aforementioned MR imaging GRE studies, these lesions can occur frequently within the relapsing phase of the disease, and consistent with others,[7] we found that lesions that become chronic active lesions can show subtle evidence of a rim at the Gd+ stage. These combined observations suggest that QSM rim+ lesions could serve as an early-stage imaging biomarker for disease prognosis, and this possibility warrants further exploration.

QSM has been shown to provide a high level of diagnostic accuracy in predicting Gd+ lesions.[13] In this study, most lesions were shell-enhancing, which are thought to be slightly older enhancing lesions and tend to demonstrate a slightly higher susceptibility.[12] Most important, the average susceptibility at the time of enhancement of all lesions (nodular and shell enhancing) was comparable with that of the previous work[12] and below the cutoff value of 13.5 ppb for predicting Gd+ MS lesions.[13] Furthermore, GRE imaging is being explored to improve the diagnostic accuracy of MS based on the identification of a central vein or central vein sign. Most interesting, we found that only one-third of lesions had a central vein on QSM, which is lower than previously suggested, using a combined T2-weighted FLAIR and T2* sequence,[33] and this finding suggests that more research is required to assess the frequency of the central vein sign in MS lesions.

There are limitations in this study. Our lesion sample size is relatively small, and more important, not all lesions were measured at each time point or followed through to all 6 years. We will continue to identify Gd+ lesions from our ongoing data base to expand on our observations and provide more data to each lesion-

age year. This expansion will allow further exploration into the effect of individual lesion size as well as patient-specific covariates such as disease duration, disability status, and treatment effect. As mentioned above, very early changes in susceptibility are likely due to a number of pathophysiologic mechanisms at play: Imaging the early-stage lesions with frequent and short-interval QSM with the addition of myelin imaging[34] would allow a more detailed analysis of the early rise in susceptibility. Similarly, a serial MR imaging study with both QSM and myelin imaging during the decay stage can evaluate the loss of iron versus remyelination in rim− lesions. Last, our study focused on white matter MS lesions and excluded cortical gray matter lesions, which are known to occur quite frequently in MS and require ultra-high-field imaging for depiction.[35] Most interesting, a high-field 7T study using QSM identified cortical lesions as having a much lower susceptibility compared with white matter lesions, suggesting less iron in cortical lesions compared with white matter lesions.[36] Thus, as we move forward with 7T QSM MR imaging, we intend to explore and compare the time-dependent susceptibility changes among smaller regions within the lesion (ie, regions of tissue enhancement) as well as lesions located within the cortex.

CONCLUSIONS

We identified unique trajectories of lesion time-dependent change in susceptibility among different subtypes of MS lesions. These observations are consistent with the iron-laden inflammatory cells present within the rim of a select subset of chronic lesions retaining iron for a number of years and slowly transitioning to an inactive state. This study supports the use of serial QSM to provide information regarding the current state of inflammation within chronic MS lesions.

Disclosures: Sandra M. Hurtado-Rúa—*RELATED*: *Grant*: National Institutes of Health, *Comments*: R01-NS104283–01A1.* Pascal Spincemaille—*UNRELATED*: *Patents (Planned, Pending or Issued)*: Cornell University, *Comments*: P.S. is an inventor on a patent describing methods (QSM) used in this work*; *Stock/Stock Options*: Medimagemetric LLC. Yi Wang—*RELATED*: *Grant*: National Institutes of Health R01NS090464, R01NS095562*; *UNRELATED*: *Patents (Planned, Pending or Issued)*: Cornell University, *Comments*: QSM technology patents*; *Stock/Stock Options:* Medimagemetric LLC, *Comments*: Cornell spinoff company. Susan A. Gauthier—*RELATED*: *Grant*: R01NS104283, R01NS105144*; *UNRELATED*: *Consultancy*: one-time Celgene Advisory Board; *Grants/Grants Pending*: Genzyme, Mallinckrodt.* Thanh D. Nguyen—*RELATED*: *Grant*: National Multiple Sclerosis Society, National Institutes of Health.* *Money paid to the institution.

REFERENCES

1. de Rochefort L, Liu T, Kressler B, et al. **Quantitative susceptibility map reconstruction from MR phase data using Bayesian regularization: validation and application to brain imaging.** *Magn Reson Med* 2010;63:194–206 CrossRef Medline
2. Wang Y, Spincemaille P, Liu Z, et al. **Clinical quantitative susceptibility mapping (QSM): biometal imaging and its emerging roles in patient care.** *J Magn Reson Imaging* 2017;46:951–71 CrossRef Medline
3. Langkammer C, Liu T, Khalil M, et al. **Quantitative susceptibility mapping in multiple sclerosis.** *Radiology* 2013;267:551–59 CrossRef Medline
4. Stuber C, Pitt D, Wang Y. **Iron in multiple sclerosis and its noninvasive imaging with quantitative susceptibility mapping.** *Int J Mol Sci* 2016;17 CrossRef Medline
5. Wisnieff C, Ramanan S, Olesik J, et al. **Quantitative susceptibility mapping (QSM) of white matter multiple sclerosis lesions: interpreting positive susceptibility and the presence of iron.** *Magn Reson Med* 2015;74:564–70 CrossRef Medline
6. Filippi M, Rocca MA, Ciccarelli O, et al; MAGNIMS Study Group. **MRI criteria for the diagnosis of multiple sclerosis: MAGNIMS consensus guidelines.** *Lancet Neurol* 2016;15:292–303 CrossRef Medline
7. Absinta M, Sati P, Schindler M, et al. **Persistent 7-Tesla phase rim predicts poor outcome in new multiple sclerosis patient lesions.** *J Clin Invest* 2016;126:2597–609 CrossRef Medline
8. Yao Y, Nguyen TD, Pandya S, et al. **Combining quantitative susceptibility mapping with automatic zero reference (QSM0) and myelin water fraction imaging to quantify iron-related myelin damage in chronic active MS lesions.** *AJNR Am J Neuroradiol* 2018;39:303–10 CrossRef Medline
9. Li JQ, Chang SX, Liu T, et al. **Reducing the object orientation dependence of susceptibility effects in gradient echo MRI through quantitative susceptibility mapping.** *Magn Reson Med* 2012;68:1563–69 CrossRef Medline
10. Zhou D, Liu T, Spincemaille P, et al. **Background field removal by solving the Laplacian boundary value problem.** *NMR Biomed* 2014;27:312–19 CrossRef Medline
11. Zhang Y, Gauthier SA, Gupta A, et al. **Longitudinal change in magnetic susceptibility of new enhanced multiple sclerosis (MS) lesions measured on serial quantitative susceptibility mapping (QSM).** *J Magn Reson Imaging* 2016;44:426–32 CrossRef Medline
12. Zhang Y, Gauthier SA, Gupta A, et al. **Quantitative susceptibility mapping and R2* measured changes during white matter lesion development in multiple sclerosis: myelin breakdown, myelin debris degradation and removal, and iron accumulation.** *AJNR Am J Neuroradiol* 2016;37:1629–35 CrossRef Medline
13. Zhang S, Nguyen TD, Zhao Y, et al. **Diagnostic accuracy of semiautomatic lesion detection plus quantitative susceptibility mapping in the identification of new and enhancing multiple sclerosis lesions.** *Neuroimage Clin* 2018;18:143–48 CrossRef Medline
14. Chen W, Gauthier SA, Gupta A, et al. **Quantitative susceptibility mapping of multiple sclerosis lesions at various ages.** *Radiology* 2014;271:183–92 CrossRef Medline
15. Bagnato F, Hametner S, Yao B, et al. **Tracking iron in multiple sclerosis: a combined imaging and histopathological study at 7 Tesla.** *Brain* 2011;134(Pt 12):3602–15 CrossRef Medline
16. Yao B, Ikonomidou VN, Cantor FK, et al. **Heterogeneity of multiple sclerosis white matter lesions detected with T2*-weighted imaging at 7.0 Tesla.** *J Neuroimaging* 2015;25:799–806 CrossRef Medline
17. Dal-Bianco A, Grabner G, Kronnerwetter C, et al. **Slow expansion of multiple sclerosis iron rim lesions: pathology and 7 T magnetic resonance imaging.** *Acta Neuropathol* 2017;133:25–42 CrossRef Medline
18. Kaunzner UW, Kang Y, Zhang S, et al. **Quantitative susceptibility mapping identifies inflammation in a subset of chronic multiple sclerosis lesions.** *Brain* 2019;142:133–45 CrossRef Medline
19. Deh K, Kawaji K, Bulk M, et al. **Multicenter reproducibility of quantitative susceptibility mapping in a gadolinium phantom using MEDI+0 automatic zero referencing.** *Magn Reson Med* 2019;81:1229–36 CrossRef Medline
20. Deh K, Nguyen TD, Eskreis-Winkler S, et al. **Reproducibility of quantitative susceptibility mapping in the brain at two field strengths from two vendors.** *J Magn Reson Imaging* 2015;42:1592–600 CrossRef Medline
21. Liu Z, Spincemaille P, Yao Y, et al. **MEDI+0: morphology enabled dipole inversion with automatic uniform cerebrospinal fluid zero reference for quantitative susceptibility mapping.** *Magn Reson Med* 2018;79:2795–803 CrossRef Medline
22. Jenkinson M, Bannister P, Brady M, et al. **Improved optimization for the robust and accurate linear registration and motion correction of brain images.** *Neuroimage* 2002;17:825–41 CrossRef Medline
23. Gaitán MI, Shea CD, Evangelou IE, et al. **Evolution of the blood-brain barrier in newly forming multiple sclerosis lesions.** *Ann Neurol* 2011;70:22–29 CrossRef Medline
24. Deh K, Ponath GD, Molvi Z, et al. **Magnetic susceptibility increases**

as diamagnetic molecules breakdown: myelin digestion during multiple sclerosis lesion formation contributes to increase on QSM. *J Magn Reson Imaging* 2018;48:1281–87 CrossRef Medline
25. Kuhlmann T, Ludwin S, Prat A, et al. **An updated histological classification system for multiple sclerosis lesions.** *Acta Neuropathol* 2017;133:13–24 CrossRef Medline
26. Frischer JM, Bramow S, Dal-Bianco A, et al. **The relation between inflammation and neurodegeneration in multiple sclerosis brains.** *Brain* 2009;132:1175–89 CrossRef Medline
27. Prineas JW, Kwon EE, Cho ES, et al. **Immunopathology of secondary-progressive multiple sclerosis.** *Ann Neurol* 2001;50:646–57 CrossRef Medline
28. Singh S, Dallenga T, Winkler A, et al. **Relationship of acute axonal damage, Wallerian degeneration, and clinical disability in multiple sclerosis.** *J Neuroinflammation* 2017;14:57 CrossRef Medline
29. Stephenson E, Nathoo N, Mahjoub Y, et al. **Iron in multiple sclerosis: roles in neurodegeneration and repair.** *Nat Rev Neurol* 2014;10:459–68 CrossRef Medline
30. Mehta V, Pei W, Yang G, et al. **Iron is a sensitive biomarker for inflammation in multiple sclerosis lesions.** *PLoS One* 2013;8:e57573 CrossRef Medline
31. Hametner S, Wimmer I, Haider L, et al. **Iron and neurodegeneration in the multiple sclerosis brain.** *Ann Neurol* 2013;74:848–61 CrossRef Medline
32. Lassmann H. **The pathologic substrate of magnetic resonance alterations in multiple sclerosis.** *Neuroimaging Clin N Am* 2008;18:563–76 CrossRef Medline
33. Maggi P, Absinta M, Grammatico M, et al. **Central vein sign differentiates multiple sclerosis from central nervous system inflammatory vasculopathies.** *Ann Neurol* 2018;83:283–94 CrossRef Medline
34. Nguyen TD, Deh K, Monohan E, et al. **Feasibility and reproducibility of whole brain myelin water mapping in 4 minutes using fast acquisition with spiral trajectory and adiabatic T2prep (FAST-T2) at 3 Tesla.** *Magn Reson Med* 2016;76:456–65 CrossRef Medline
35. Magliozzi R, Reynolds R, Calabrese M. **MRI of cortical lesions and its use in studying their role in MS pathogenesis and disease course.** *Brain Pathol* 2018;28:735–42 CrossRef Medline
36. Bian W, Tranvinh E, Tourdias T, et al. **In vivo 7T MR quantitative susceptibility mapping reveals opposite susceptibility contrast between cortical and white matter lesions in multiple sclerosis.** *AJNR Am J Neuroradiol* 2016;37:1808–15 CrossRef Medline